

XAS Study of Multifunctional Magnetic Solid Lipid Nanoparticles Containers for Combined Medical Therapies

Iron oxide nanoparticles (IONPs) are commonly studied as biomedical tool by their improved biocompatibility against other magnetic nanoparticles [1]. One strategy to improve the chemical stability of such nanoparticles and, in some cases enhance its magnetic properties, is the conjugation with functional coatings [2]. The conjugation with lipidic molecules to form solid lipid compounds provides to the hybrid system not only a higher biocompatibility but also the possibility of attaching therapeutical biomolecules [2]. In the present proposal, the IONPS are conjugated with phospholipidic molecules (i.e. *glyceryl laurate*), forming solid lipid nanoparticles (SLNPs) by a microemulsion method [3]. Such SLNPs are designed to be multi-funtional tools: carrying drugs to selected targets by magnetic guidance and also be suitable in hyperthermia therapies. For both purposes, the magnetic features of these hybrids must be perfectly characterized and controlled. In this way, previously studies [4] have demonstrated us that the subsequent treatments carried out for functionalize the IONPs are dramatically determinant in the magnetic performance of such NPs. i.e. Some of such hybrid particles have been characterized magnetically, displaying a complex magnetic behaviour which is not possible to be explained only by aggregation-disaggregation processes, but by complex magnetic and chemical interactions in the NP shell. in the conjugation are determinant [5] in obtaining the best performance of these SLNPs to be implemented as nanocarriers and hyperthermia tools.

The as-obtained IONPs, FeOS, are first observed by TEM. NPs with very low size dispersion are obtained with diameters of circa 7 nm. The image depicted

in figure 1 is a representative image of a dried sample of IONPS in which the high monodispersity can be observed.

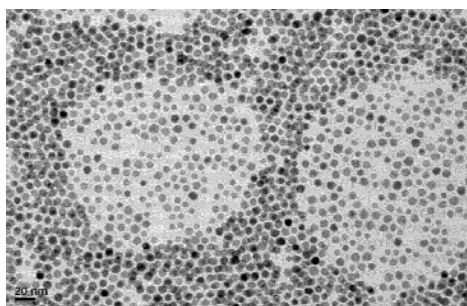


Figure 1. TEM image of the uncoated FeOS

The first magnetic characterization is carried out in the SQUID, obtaining the FC and ZFC of the aqueous SLNPS samples and reference FeOS in CH₃Cl. Both curves, FC and ZFC, are depicted in Figure 2 for each group of samples. The FeOS (fig. 2.a) present a blocking temperature (BT) nearby 32 K, where the maximum displays a wide shape, revealing the existence of energy barriers for spin inversion. The wideness of the relative maximum is related to the existence of interparticle dipolar interactions. The proximity of the BT and the irreversibility temperature (IT) also reflects the narrow distribution of NP sizes observed by TEM. After the conjugation into SLNPS the BT values decrease for both conjugates, below 23 K (Fig.2.b&c.). This behaviour could reveal the disaggregation effect of the lipidic matrix in the IONPS respect to non-conjugated ones, reducing the inter-particle interaction: the BT is reduced by effect of the disaggregation of the original nanoparticles inside the lipidic matrix. In case of FeOS@gly the BT falls to 17 K, and following the argument of the reduction of interparticle interaction by disaggregation, could be related with slight differences in the hydrophobicity and hydrodynamic size (51 and 52 nm, respectively) in both compounds.

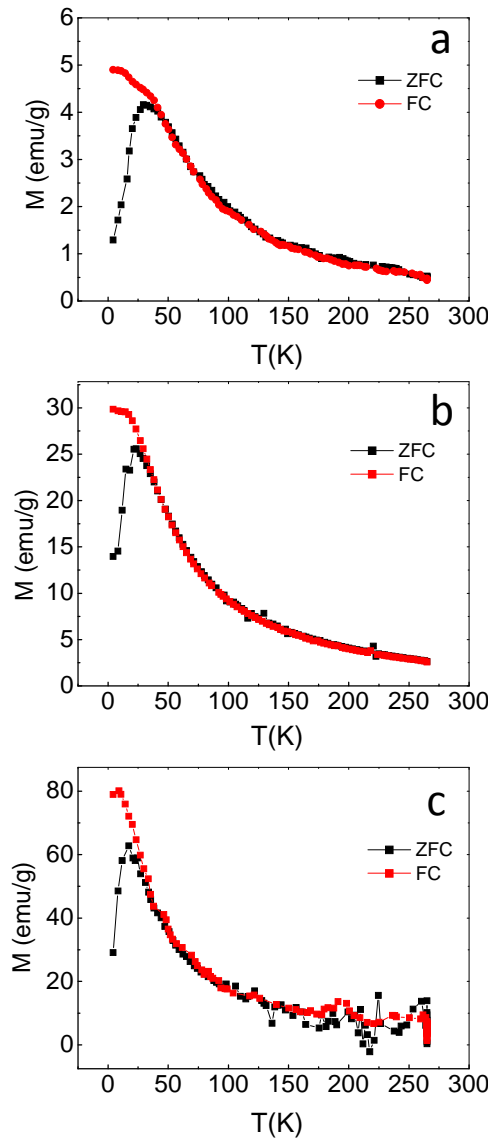


Figure 2. Magnetization curves upon field curve (FC) and Zero field curve (ZFC) for the studied magnetic samples a) FeOS, b) FeOS@gly and c) FeOS@ste.

Magnetic field-dependent magnetization curves ($M(H)$) from these SLNPS and IONPS are obtained at 5K and RT, are depicted in figure 3. Inset in each curve shows the corresponding low field region detail. Starting IONPS presents magnetization values of 20 emu/g at 5K and 12 emu/g at RT, low values if compared with equivalent maghemite/magnetite magnetic nanoparticles. The

uncoated FeOS NPs display coercivity values of 115.7 Oe obtained from the low temperature cycles, with ferromagnetic features in both RT and low temperature conditions. In case of coated SLNPs, RT cycles shows paramagnetic behavior, with coercivity values at 5K of 100.7 and 63.2 Oe, respectively for FeOS@ste and FeOS@gly (Figure 4). This sensitive reduction in coercivity for the coated matches well with the hypothesis of the disaggregation of particles by the coating. The paramagnetic behaviour at RT in the coated particles must be generated by the paramagnetic signal of the lipidic coating that surrounds the NPs which is vanished at low temperatures.

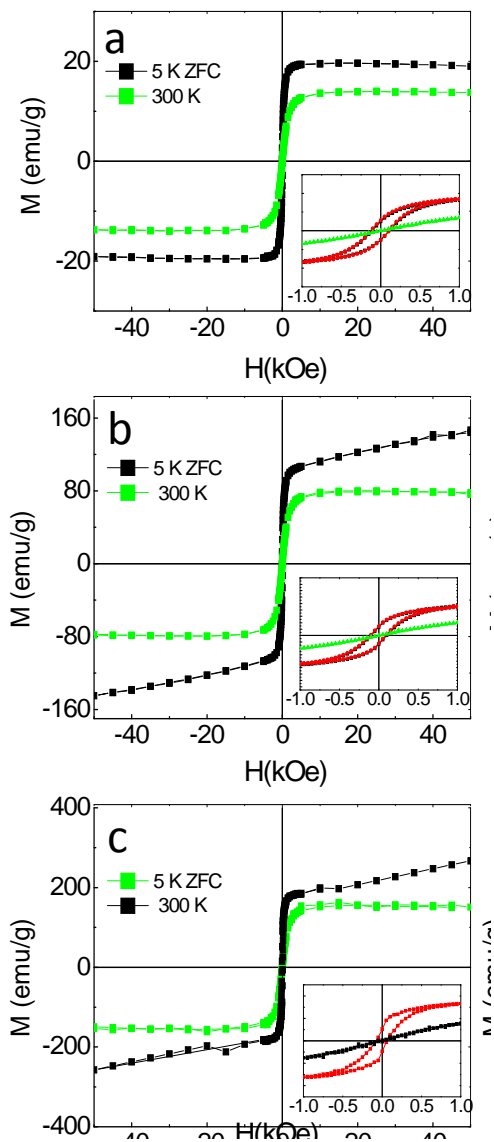


Figure 3. SQUID Magnetization curves vs. applied magnetic field for the studied magnetic nanoparticles a) FeOS, b) FeOS@gly, c) FeOS@ste at 5 and 300 K.

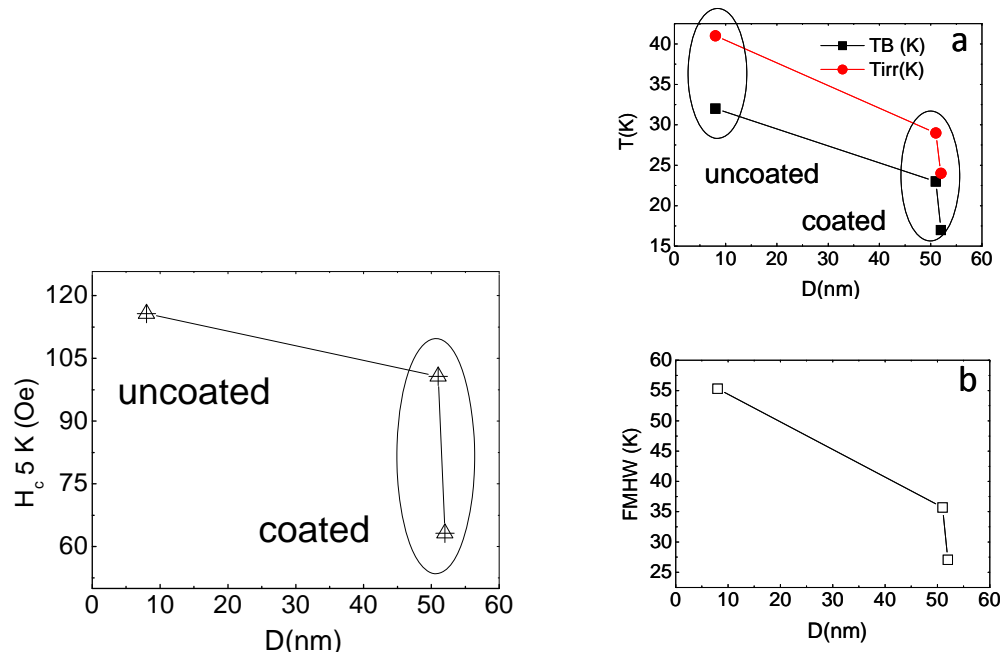


Fig 4. Coercive field, blocking and irreversibility temperatures and FWHM of the ZFC measured for the magnetic particles

To evaluate the plausible origin of the modification of magnetism, and for determine the electronic state of Fe in the SLNPs we have performed XAS measurements in the XANES regime. Fig 5 shows XANES spectra of the Fe oxide references and a dried sample of original FeOS nanoparticles. The oxidation state of iron in the references changes from 2 for FeO to 3+ for γ -Fe₂O₃ and α -Fe₂O₃. Considering the energy edge as the first peak of the derivative of XAS signal and linearity between the energy shift and the oxidation state (Kuntz law¹, Fig.5.b), these results indicate that the iron in the sample are nominally in the 2.9+ formal oxidation state, that is, slightly under that corresponds to maghemite (formally 3+) and clearly over to the magnetite's

(2.67+). However, both the shape of the main absorption edge peak (white line) and of the second maximum (shoulder) resembles more to Fe₃O₄ spectra. Other similarities with magnetite are also observed in the derivative feature (not showed).

Regarding the feature of the pre-peak, that is due to transitions 1s→3d in hybridized 3d-4s levels and is characteristic for Fe in spinel structures, displays a quite different shape in FeOS than the observed in magnetite and maghemite. The prepeak is slightly shifted to lower energy and presents less intensity, contrary to expected for a Fe oxide (case of supposing magnetite/maghemite composition) in a nanoparticle form by the increase of the surface/volume ration. Both the reduction of the oxidizing state and the pre-peak feature could leads to suppose a configuration of nanoparticle with complex structure, such as a core-shell.

For the Fe contained in the SLNPs a set of XANES spectra has been also obtained (fig 5.c). In these XANES measurements the main feature is the absence of significant modification in the oxidation state, by comparing the position of the absorption edge. This comparison is clearer by using the first derivative in the edge (inset in Fig.5.c), that shows no displacement between spectra of the initial IONPs and the SLNPS. The shape of the spectra in the white line present similar features but a increase in intensity in this zone is observed for the SLNPs and should be related to modifications in the surface chemistry of the Fe in the coated NPs as commonly describes as shape resonances [2]. This resonances should rise the mean peak of the whiteline, which would be more pronounced the larger were the number of CO groups bounded to the Fe atoms. As Glycerol molecule has more content in such kind of bounds we could suppose that this should yield to a more intense peak than the observed in stearic acid in XANES spectra.

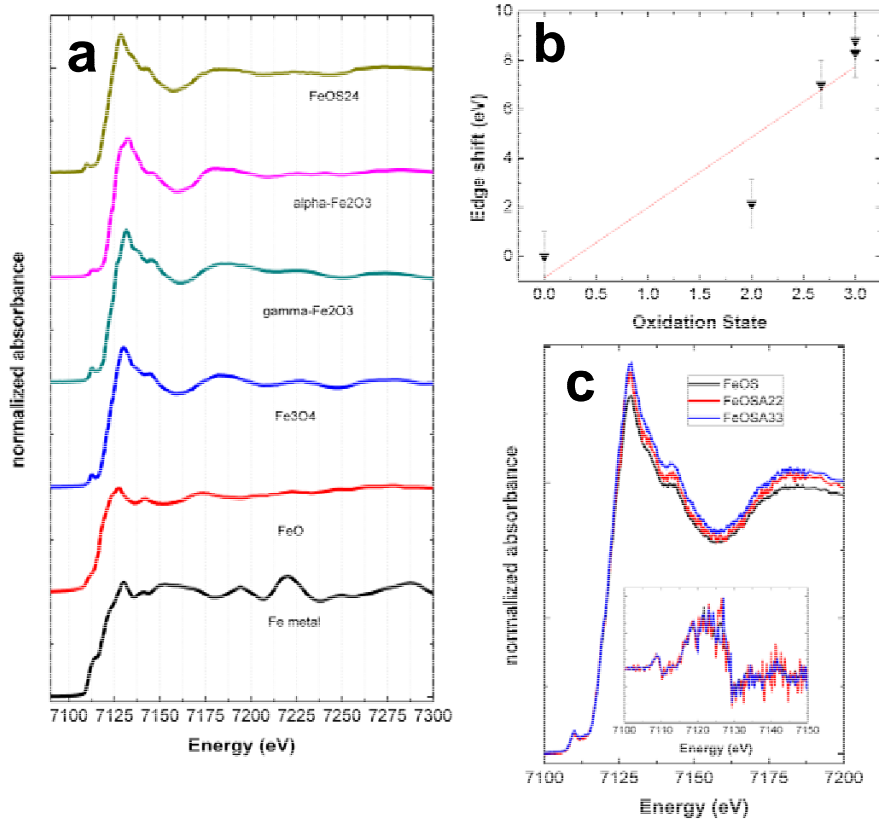


Fig 5. a) XAS spectra of the metallic Fe, Fe oxides and FeOS samples; b) representation of the energy shift of the absorption edge as a function of the formal oxidation state of the references (Kunzl's law); c) XANES spectra of the FeOS and SLNPs, the inset shows the derivative of the absorption spectra in the edge zone for the same samples.

The oscillations observed in the films and their corresponding Fourier transforms (FT) are compared with those of the spinel references (Fig.6). Two major peaks corresponding to the two first shells of the Fe neighbor atoms dominate these Fourier transforms, which are characteristics of the spinel geometry structure.^{3,4} Regarding the relative intensity and shape of the peaks, the selected model to build the shell structure for simulations is the corresponding to magnetite. Following this model, the first peak is attributed to the Fe-O coordination in the first shell of Fe atoms. The second peaks belong to the second shell of Fe atoms, which is more complex with different Fe-Fe

coordination. Both average distances comprise tetrahedral and octahedral positions of Fe in the structure, and they differ due to a variation in the occupancies and vacancies. A summary of the shell distances, occupancies and Debye-Waller factor estimated for each coordination shell is listed in Table 1 for the magnetite reference and to the studied samples. While Fe-O distance in the first shell is 1.96 Å in fitted values for magnetite, this distance is shortened in the uncoated FeOS and FeOS@ste samples (1.94 Å) and very similar in the FeOS@gly(1.97Å). Nevertheless such small differences could be attribute to the experimental uncertainty (of 1%). Considering this range of uncertainty, the differences in the position of the subsequent atomic shells can be considered equivalent between the samples and to the magnetite reference.

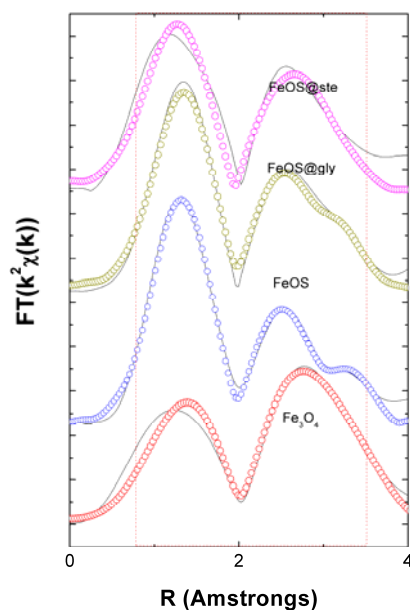


Fig 6. EXAFS corresponding Fourier transforms (FT) of FeOS, FeOS@gly and FeOS@ste samples and Fe₃O₄ reference. The FTs were performed in the range $k=2.50-9 \text{ \AA}^{-1}$ with k^2 weighting in the oscillation.

sample	Shell	R (Å)	N	$\Delta\sigma$ (Å ⁻¹)
Fe ₃ O ₄	Fe-O	1.96	3.6	$1 \cdot 10^{-2}$

	Fe-Fe	3.02	5.8	$9 \cdot 10^{-3}$
	Fe-Fe	3.54	3.2	$9 \cdot 10^{-3}$
FeOS	Fe-O	1.94	2.3	$2 \cdot 10^{-3}$
	Fe-Fe	3.00	1.8	$2.0 \cdot 10^{-2}$
	Fe-Fe	3.60	0.8	$2.0 \cdot 10^{-2}$
FeOS@gly	Fe-O	1.97	3.3	$1 \cdot 10^{-2}$
	Fe-Fe	2.98	1.2	$1.2 \cdot 10^{-3}$
	Fe-Fe	3.61	0.8	$1.2 \cdot 10^{-3}$
FeOS@ste	Fe-O	1.94	3.8	$1.4 \cdot 10^{-2}$
	Fe-Fe	3.09	1.8	$1.1 \cdot 10^{-2}$
	Fe-Fe	3.53	0.4	$1.1 \cdot 10^{-2}$

Table 1. Summary of the fitting parameters for the shell position, occupancy and Debye-Waller factor of the FeOS samples and magnetite reference.

However, more interesting differences arise from the occupancy of the atomic shells. First, the O amount in the first coordination shell in the FeOS sample compared to the magnetite is clearly larger, as shorter is the mean Fe first and second neighborhood. This relative decrease in the coordination number could be a consequence of the finite size of the NPs respect to the magnetite reference. In the uncoated FeOS nanoparticles regarding the relative mean coordination number of the second and third shells (corresponding to Fe atoms) there is a relative decrease of Fe respect to the O amount of the first shell compared to magnetite. This relative decrement of the Fe content in the first neighborhood of the Fe should be related with the larger formal oxidation state observed in the XANES for these samples respect to magnetite. This tendency in decrease the relative Fe neighborhood is not observed in the lipid coated FeOS samples, and should be related to the chemical bonding of the outer Fe atoms with the lipidic molecules. This fact should increase the nominal value of O surrounding the Fe respect to non coated NPs, that is quantitatively observed by the nanoscopic

size of the nanoparticles systems. In case of FeOS NPs the mean neighborhood occupation ratio Fe-Fe/Fe-O (first shell) is 0.78, but for the FeOS@gly and FeOS@ste are 0.36 and 0.47, respectively. This values give an estimation of the increase in O on the surface respect to the uncoated NPs.

The question of why the coated SLNPs keeps the formal oxidation state in reference to the uncoated should be addressed to the low relevance of the surface atoms oxidation state in the global oxidation state of the particle, beyond the finite size effect. The presence of a oxidized layer in the surface by bonding with the organic molecules could explain this observation, but the composition of such layer must not be too different to an spinel as the minimum variations in the shape of the EXAFS and XANES spectra show. This layer should be composed by ferromagnetic or paramagnetic structures as the lack of Exchange Bias points out. Thereby, a maghemite or paramagnetic-like Fe composite should cover the coated NPs.

Conclusions

Micro-emulsion method allows the fabrication of solid lipid nanoparticles consisting of a magnetic load in form of magnetic iron oxide nanoparticles inside them. This processing method permits the successful dispersion of the NPs inside the SLNPs avoiding the aggregation of the magnetic particles and thus reducing the dipolar interactions between individual NPs. This feature enhances the superparamagnetic feature of these conjugates respect to the initial IONPS. Moreover, due to their increased size these SLNPS present larger magnetic momentums.

The measures during the experiment carried out in the ESRF has improved substantially our knowledge in the chemical and magnetic structure of the SLNPs and the relationship with the synthesis conditions.

References

- ¹ V. Kunzl, V. Collect. Trav. Chim. Techcolovaquie 1932, 4, 213.
- ² A. Bianconi, M. Dell'Araccia, P. J. Durham and J. B. Pendry Multiple-scattering resonances and structural effects in the x-ray-absorption near-edge spectra of Fe II and Fe III hexacyanide complexes" Phys. Rev. B 26, 6502–6508 (1982)
- ³ L. Signorini, L. Pasquini, L. Savini, R. Carboni, F. Boscherini, E. Bonetti, A. Giglia, M. Pedio, N. Mahne and S. Nannarone, Phys. Rev. B 68, 195423 (2003).
- ⁴ A. Corrias, G. Ennas, G. Mountjoy and G. Paschina. Phys. Chem. Chem. Phys. 2, 1045 (2000)